

# Magnetic polarity stratigraphy of Plio–Pleistocene Pinjor Formation (type locality), Siwalik Group, NW Himalaya, India

V. Kumaravel, S. J. Sangode\*, Rohtash Kumar and N. Siva Siddaiah

Wadia Institute of Himalayan Geology, 33, General Mahadeo Singh Road, Dehradun 248 001, India

**Pinjor (near Chandigarh) is the only type locality in India for the Siwalik Group. We present here, the magnetic polarity stratigraphy of two sections (Ghaggar river and Moginand Nalla) from this area and propose the Ghaggar section for consideration as a standard stratigraphic section for the Pinjor Formation of the Siwalik Group. A total of 83 oriented sites from the 1030 m thick Ghaggar section give an age estimate of ~2.7 to ~0.5 Ma and 23 sites from 310 m thick Moginand section deduce an age estimate of ~2 to ~0.86 Ma. The continuously exposed Ghaggar river section has been previously well documented using sedimentology, biostratigraphy and palaeoecology. A fission track age of  $2.14 \pm 0.5$  Ma on the volcanic ash in the Ghaggar river section coincides with the Gauss–Matuyama polarity reversal (2.58 Ma) constraining the lower limit for the Pinjor Formation. Occurrence of the Lower Boulder Conglomerate Formation at ~1.79 Ma marks the upper boundary for the Pinjor Formation that coincides with the Plio–Pleistocene boundary. The thermal demagnetization spectra uniquely reveal the predominance of a uni-component system, resulting in a better clustering of the magnetostratigraphic data (normal mean  $D = 8.2^\circ$ ,  $I = 27.0^\circ$ ,  $\alpha_{95} = 8.8^\circ$ ; reverse mean  $D = 167.4^\circ$ ,  $I = -25.9^\circ$ ,  $\alpha_{95} = 6.9^\circ$ ). With the present magnetostratigraphic time constraints, the Ghaggar section forms an ideal location for more interdisciplinary studies along the Plio–Pleistocene boundary in the Himalaya and may be considered as a standard stratotype section for the Pinjor Formation of the Siwalik Group.**

STANDARD stratigraphic records of major climatic changes such as Plio–Pleistocene (~ 1.77 Ma) provide a laboratory for interdisciplinary approaches to understand the natural processes. There is little documentation of such records from the Indian subcontinent. The Pinjor Formation of the Siwalik Group witnessed the Plio–Pleistocene tectonic and climatic changes in the Himalayan Foreland Basin (HFB). The Pinjor area near Chandigarh has been marked as the type locality for the Pinjor Formation of the Siwalik Group way back in 1913 by Pilgrim<sup>1</sup>. However, little attention has been paid to highlight any stratotype section for this only type locality of the Siwalik Group available in India.

In this context we attempt magnetic polarity stratigraphy of one of the well exposed sections (the Ghaggar river section) and its extension to Moginand Nalla (about 4 km eastward). A magnetostratigraphic correlation has also been established to previously dated Patiali Rao<sup>2</sup>, Khetpurali<sup>3</sup> and Haripur Khol<sup>4</sup> sections stretching over an area of about 60 km in the Subathu sub-basin of the HFB.

## The Siwalik Group

The Siwalik Group comprises more than ~6000 m thick freshwater molasse sediments, thus providing an opportunity to study sedimentation, palaeoclimate and tectonic processes<sup>5–7</sup> in the HFB for the past ~18 Ma. The Siwalik Group is divided into the Lower, Middle and Upper Siwalik subgroups based on the faunal assemblages and lithofacies variations<sup>1,7,8</sup>. The Lower Siwalik Subgroup (~18 to ~11 Ma) comprising Kamlial and Chinji Formations is characterized by first appearance of *Girafiddae* and the depositional environment of high sinuosity meandering streams with broad floodplains<sup>7</sup>. At outcrop level, the Lower Siwaliks comprise highly indurated, fine to medium-grained, grey to greenish-blue and purple sandstones interbedded with reddish-brown to grey and hard concretionary mudstones and palaeosols. These are also characterized by the appearance of staurolite in the heavy mineral assemblage<sup>6</sup>. The type localities for the Lower Siwalik Subgroup are described from the Kamlial and Chinji villages of Pakistan in the Potwar Plateau. The Middle Siwalik Subgroup (~11 Ma to 5.23 Ma), subdivided into the Nagri and Dhok Pathan Formations records first appearance of the fossil *Hipparion* and appearance of the heavy mineral kyanite<sup>6</sup>. The Nagri Formation (~11 to 8.5 Ma) is characteristic of ‘salt and pepper’ textured, grey sandstones mainly deposited in braided channels<sup>7</sup>. The Dhok Pathan Formation records the predominance of mudstone and palaeosol facies. The Upper Siwalik Subgroup comprises Tatrot Formation (~5.26 to ~2.5 Ma), Pinjor Formation (~2.5 to ~1.7 Ma) and Boulder Conglomerate Formation (~1.7 to ~0.5 Ma). The Upper Siwaliks are characterized by the appearance of heavy minerals, sillimanite and hornblende<sup>6</sup>. Appearance of the fast-invading or migratory forms of Pinjor fauna (e.g. *Equus*, *Camelus*)<sup>1</sup>, is the characteristic faunal change in the Upper Siwalik Subgroup.

\*For correspondence. (e-mail: Sangode@rediffmail.com)

All the type localities of Siwalik formations except Pinjor are described from the Potwar Plateau. The type locality of the Siwalik Group lying in the Indian counterpart occurs near Chandigarh<sup>1</sup>, characterized by a large collection of Pinjor fauna<sup>9,10</sup>. Few isolated biostratigraphic<sup>9-14</sup> and magnetostratigraphic<sup>2-4,15,16</sup> attempts have been made in the area. Biostratigraphic and palaeoecological attempts are still based upon indefinite chronology due to the absence of chronologic order like that given by magnetostratigraphy. On the other hand, magnetostratigraphic attempts too are based on uncertainties due to the absence of independent benchmarks. Tandon and Kumar<sup>17</sup> reported a volcanic ash bed in the Ghaggar river section, NE of Chandigarh. Using fission track, Mehta *et al.*<sup>18</sup> dated it around 2.14 ± 0.5 Ma. Recently, Patnaik<sup>11</sup> highlighted the palaeoecological significance of rodent occurrences from this section. Previously, Kumar and Tandon<sup>19</sup> attempted detailed sedimentology of this section based upon facies analysis, sedimentation pattern and geometry. Availability of this interdisciplinary information, its easy access and continuous nature of the section prompted us to attempt magnetic polarity stratigraphy in this type locality for Pinjor Formation. An eastward magnetostratigraphic extension has been made by attempting the Moginand section. In this article, we further

attempt to correlate the previously dated coeval sections within the sub-basin to document the major lithological boundaries, lateral variation in rate of sedimentation and lithofacies.

### Area of study and geological settings

The HFB is sub-divided into several smaller basins based on the subsurface highs and lineaments<sup>20,21</sup>. The Subathu sub-basin, where the study area falls, represents the central part of the HFB; it is confined by the Yamuna tear fault in the east and the Fugal–Manali lineament in the west<sup>22,23</sup>. The studied sections are located NE of Chandigarh near Panchkula along the Ghaggar and Moginand rivers (Figure 1). The area is marked by the Himalayan Foreland Thrust in the south and Nahan Thrust in the north. The Upper Siwalik sequence that includes Pinjor, Lower Boulder Conglomerate and Upper Boulder Conglomerate Formations is well exposed more continuously along the Ghaggar section than the Moginand section. Lithostratigraphy, fossil occurrences and sedimentological features from the Ghaggar (Figure 2) and Moginand sections (Figure 3) are summarized in Tables 1 and 2.

**Table 1.** Major lithological variations with age constrains for the Ghaggar section of the Upper Siwalik Subgroup

Formation and thickness	Lithological details (average thickness in parenthesis)	Contact relationship	Diagnostic fauna <sup>1,10,11,12,14</sup>	Depositional environment
Upper Boulder Conglomerate (330 m) ~1.2 to ~0.5 Ma Pleistocene	Thickly bedded massive conglomerates (5–20 m) with pebbles, cobbles and boulders embedded in sandy to silty matrix and interstratified sandstones (~4 m) and mudstones (2–11 m)	Thrust contact with the (Nahan Thrust) physically overlying Lower Siwalik Subgroup	Not recorded	Proximal fan region, debris flow at places
Lower Boulder Conglomerate (245 m) ~1.79 to ~1.2 Ma Pleistocene	Brown to greyish-brown, fine, medium to coarse-grained sandstones (2–7 m) with pebbles and brown mudstones (~6 m) and pedogenic horizons (~1–5 m), well-imbriated, stratified conglomerates (1–7 m) with large-scale cross stratifications	Upper contact with the Upper Boulder Conglomerate is transitional; alterations of mudstones, sandstones and conglomerates transitionally pass into thick and massive Boulder Conglomerate	Not recorded	Braided river channel and proximal alluvial fan
Pinjor Formation (380 m) ~2.6 to ~1.79 Ma Upper Pliocene	Brown to greyish-brown, fine, medium and coarse-grained sandstones (0.5–4 m), multi-storey sandstones (~9 m), pebbly sandstones, pedogenic and non-pedogenic overbank facies (2–15 m)	Upper contact with the Lower Boulder Conglomerate is transitional; pebbly beds gradually increase; sandstone and mudstone beds gradually decrease	<i>Dilatomy</i> sp.; <i>Talera pinjoricus</i> ; <i>Mus linmaeusi</i> ; <i>Stegodon insignis</i> ; <i>Archidiskodon planifrons</i> ; <i>Elephas hysudricus</i> ; <i>Equus sivalensis</i> ; <i>Leptobos</i> and <i>Bos</i>	High gradient, low sinuosity streams, mainly of piedmont drainage system
Tatrot Formation (>60 m) ~>2.6 Ma Middle Pliocene	Fine, medium and coarse-grained, grey sandstones, variegated mudstones and siltstones	Upper contact with the Pinjor Formation is transitional; grey beds in the transitional zone gradually disappear and brown sandstone and mudstone become prominent; Lower contact is not exposed	<i>Stegodon bombifrons</i> ; <i>Pentalophodon khetpuralensis</i> ; <i>Hipparion antelopinum</i> ; <i>Hexaprotadon sivalensis</i> ; <i>Hipparion theobaldi</i> ; <i>Camelus sivalensis</i>	Low sinuosity streams; mainly of trunk river system

**Table 2.** Major lithological characters with age constrains for the Moginand section of the Upper Siwalik Subgroup

Formation and thickness	Lithological details (average thickness in parenthesis)	Diagnostic fauna <sup>1,10-12,14</sup>	Depositional environment
Lower Boulder Conglomerate (>64 m) (~< 1.1 Ma) Pleistocene	Medium to coarse-grained sandstones with pebbles (1–6 m), brown mudstones (~8 m), well-stratified conglomerates (0.5–2 m)	Not recorded	Braided river channel and proximal alluvial fan
Pinjore Formation (246 m) (~2 to 1.1 Ma) Plio–Pleistocene	Fine, medium to coarse-grained grey and buff-coloured sandstones (1–5 m), multistorey sandstones (~10 m) with erosional scours and TCS, brown mudstones (0.5–3 m), yellowish to brownish podogenic horizons (~5 m) with concretions	<i>Dilatomy</i> sp.; <i>A. planifrons</i> ; <i>E. hysudricus</i> ; <i>E. sivalensis</i> ; <i>Leptobos</i> and <i>Bos</i>	High gradient, low sinuosity streams, mainly of piedmont drainage system

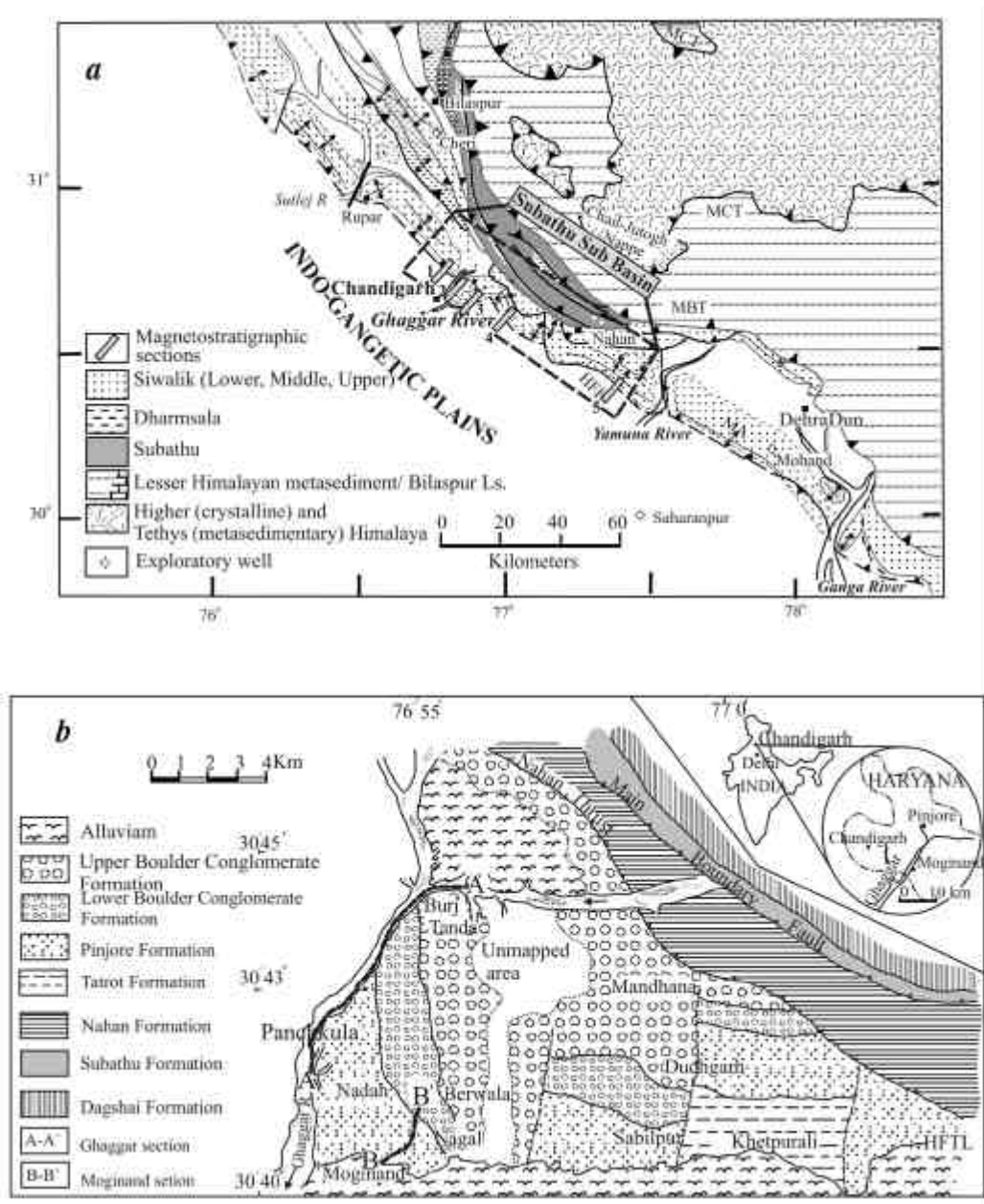


**Figure 1.** a, Geological map of the Subathu sub-basin showing different lithostratigraphic and tectonic units. Location of the studied section is shown in rectangular area. 1, Patiali Rao; 2, Ghaggar; 3, Moginand; 4, Khetpurali and 5, Haripur section. (Compiled after Karunakaran and Ranga Rao<sup>27</sup>, Raiverman *et al.*<sup>28</sup> and Powers *et al.*<sup>29</sup>). b, Geological map of the study area. Traverses for the studied sections are indicated by broken lines (after Kumar and Tandon<sup>19</sup>).

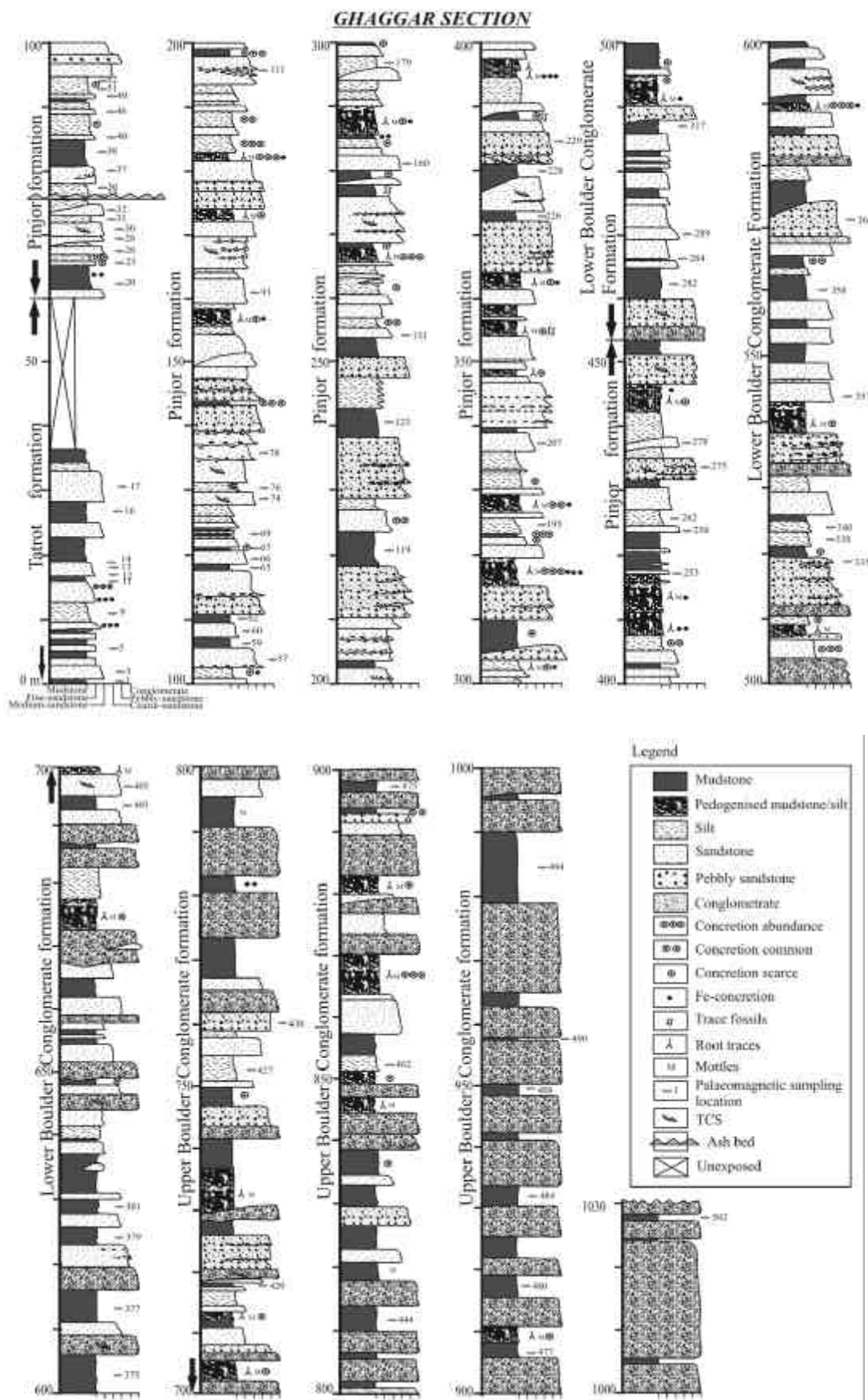


**Figure 2.** Detailed litholog of the measured section of the Upper Siwalik Subgroup in the Ghaggar river.

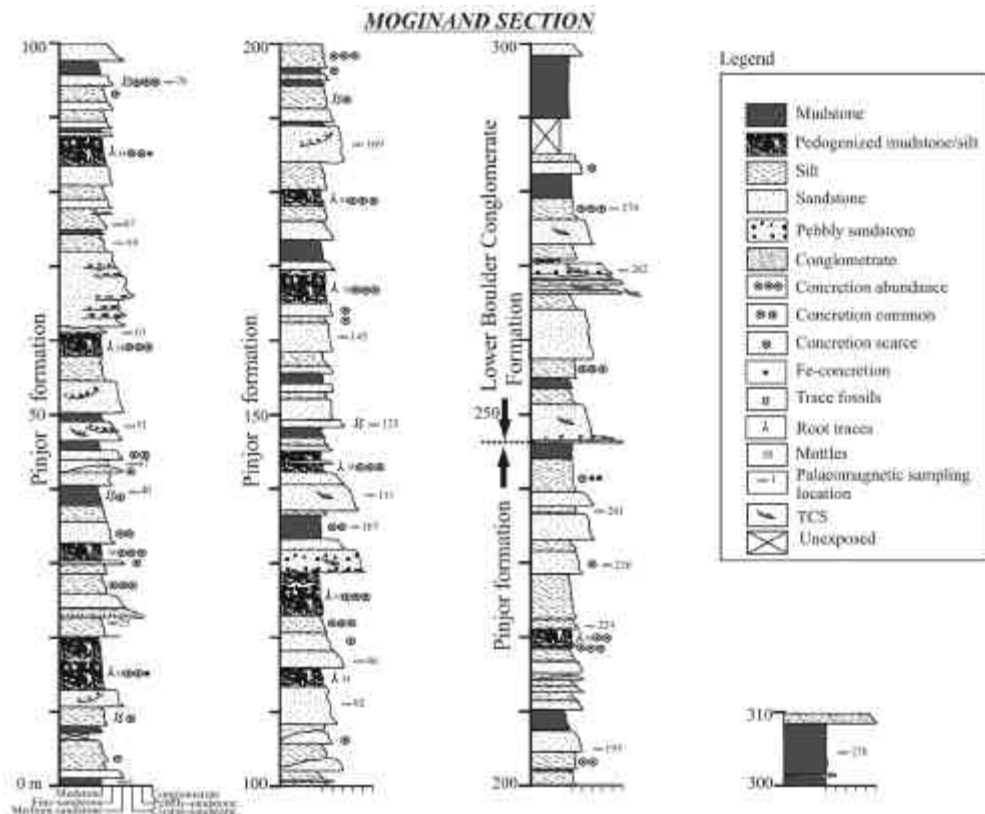


Figure 3. Detailed lithology of the measured section of the Upper Siwalik Subgroup in the Moginand river.

## Magnetic polarity stratigraphy

### Sample collection

Oriented blocks for palaeomagnetic studies were collected from 83 sites in the Ghaggar section (Figure 2) and 23 sites in Moginand section (Figure 3) using standard methods<sup>24</sup>. Preferably fine sediments like silt, mudstone and overbank clay facies were collected in order to get more reliable palaeomagnetic data from stable single domain grains avoiding the zones of pedogenically altered and disturbed beddings. The oriented samples have been drilled (hard samples) and cut (soft samples) into 2.5 cm cylindrical and cubic shapes. The soft mudstone samples were finished on sandpaper and finally thin fevicol coating was given for dust-proof handling.

### Palaeomagnetic analysis

Initial susceptibility measurement was carried out on Bartington magnetic susceptibility meter – MS2B, the progressive thermal demagnetization was carried out using Magnon International TD-800 thermal demagnetizer and the remanance measured on Schonstedt Digital Spinner Magnetometer (DSM-2). A total of 58 samples were selected randomly throughout the section for pilot demagnetization study in order to, (i) understand the remanant component

assemblage, (ii) study the changes in the vector direction during demagnetization, and (iii) monitor the intensity decay and change in the initial magnetic susceptibilities for identification of characteristic remanant magnetization. Partial thermal demagnetizations were carried out at the temperature intervals of 50 and 100°C up to 700°C with continuous monitoring of magnetic susceptibility. After demagnetizing at any particular temperature, the sample was cooled to room temperature in the near-zero magnetic field (~5 nT) and analysed in the DSM-2 to find out the  $D$ ,  $I$  and intensity of the natural remanance magnetizations.

Results of the partial thermal demagnetization are plotted in the Vector End Point (VEP) diagrams/Zijderveld diagrams (Figure 4). The trajectory of the magnetic vectors in the VEP reflects the changes in  $D$ ,  $I$  and intensity during demagnetization with removal of subsequently harder components. All the VEPs are displayed on two orthogonal planes, i.e. solid circles onto the horizontal plane and open circles onto the vertical plane<sup>25</sup> (Figure 4). The demagnetization analysis for the Ghaggar and Moginand samples reveals substantially weak secondary components. A brief description of vector behaviour for representative samples is given below.

The sample GH35 (Figure 4) records the removal of viscous component at ~100°C and a secondary component was cleaned at ~400°C, after which the trajectory takes a linear path towards the origin. Increase in the intensity

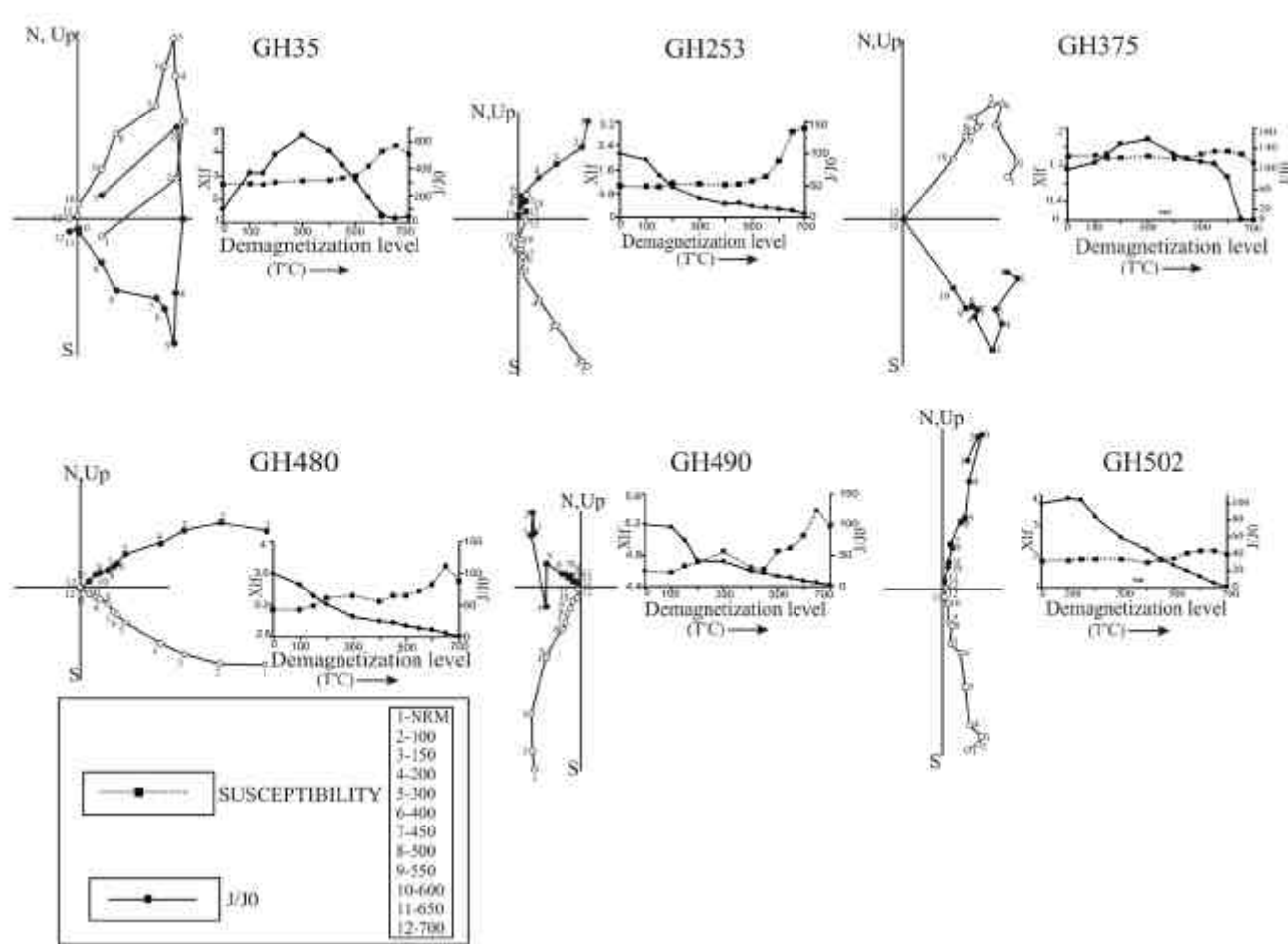


**Figure 4.** Vector End Point (VEP)/Zijderveld plots for representative samples. Solid circles are VEP projections on the horizontal plane and open circles indicate projections on the vertical plane (see text for details).

from 0 to 300°C is due to removal of high-angle secondary component (see the acute angle at stage 5 (= 300°C) in Figure 4). The acute angle at 300°C indicates the non-overlapping coercivity spectra. The sample GH253 shows predominance of single component with a viscous component demagnetized below 150°C (Figure 4). The sample GH375 indicates removal of distinct secondary component below 300°C and then the linear decay after 500°C characterizing primary component (ChRM). The sample GH480 shows predominance of single component decaying towards the origin (Figure 4). The sample GH490 shows drop in intensity and change in direction at 200°C, indicating weak non-overlapping secondary component unblocked around 200°C. Although there is an increase in the magnetic susceptibility after 450°C, the intensity decay is linear probably indicating laboratory oxidation of poorly crystalline iron oxides, those not affecting the primary remanence (Figure 4). The sample GH502 shows removal of viscous component at 150°C and the vector trajectories move towards the origin, indicating predominance of single component (Figure 4). To summarize, majority of the samples from the Ghaggar and Moginand sections have indicated

predominance of single component that decays linearly to the origin, suggesting primary/ChRM direction.

#### Age estimation

The site mean direction (after bedding/tilt correction), resultant vector ( $R$ ), precision parameter ( $k$ ), angular dispersion ( $s$ ), confidence limit ( $\alpha$ -95% and  $\alpha$ -63%) for each bed were calculated using derivatives given in Butler<sup>25</sup>. Finally, the Virtual Geomagnetic Pole (VGP) latitude of each horizon is plotted against the measured litho-column to reconstruct the local magnetic reversal pattern (Figure 5). The positive and negative values of the VGP latitude indicate respective normal and reverse polarity of the geomagnetic field<sup>25</sup>. These magnetic reversals are correlated with Geomagnetic Polarity Time Scale (GPTS) of Cande and Kent<sup>26</sup>, using the benchmark of volcanic ash occurrence at  $2.14 \pm 0.5$  Ma. Sum of four normal and three reverse magnetozones is obtained for the Ghaggar section, and two normal and three reverse for Moginand section (Figure 5). Thus, the GPTS-correlated ages of the Ghag-

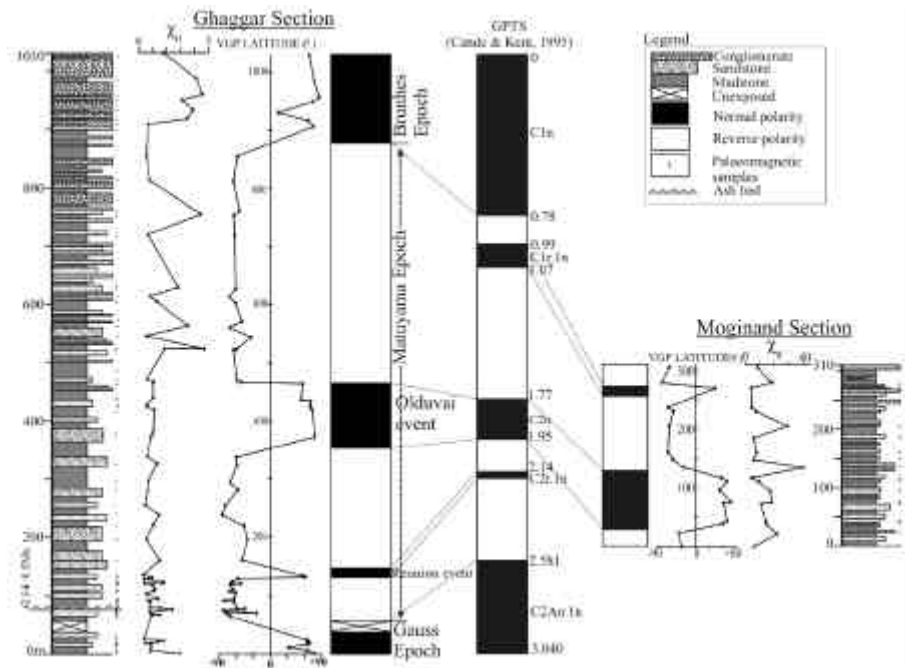


**Figure 5.** Magnetostratigraphic plots of the Ghaggar and Moginand sections. Virtual geomagnetic pole latitudes are plotted against the measured litho-column and the observed magnetic polarity. Chron and sub-chrons are correlated with the geomagnetic polarity timescale<sup>26</sup>. Magnetic susceptibility plot shows relative variation in susceptibility throughout the section.

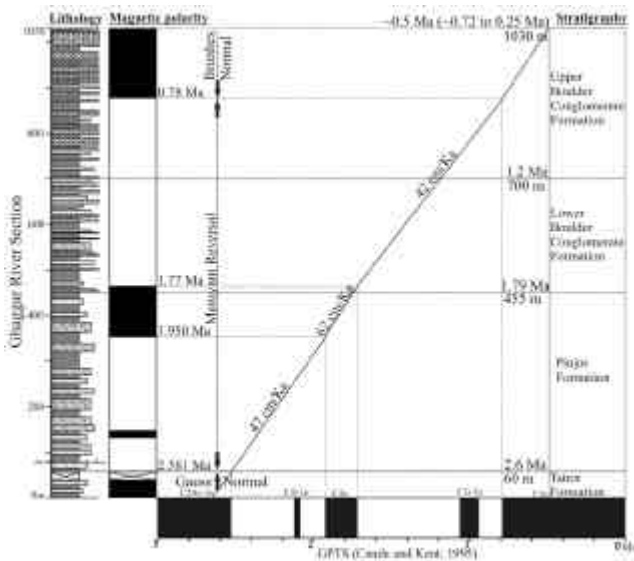


**Figure 6.** Geomagnetic polarity timescale versus stratigraphic thickness of the Upper Siwalik sediments in the Ghaggar section showing Sediment Accumulation Rate (SAR). Note the rapid rise in SAR at Olduvai times (1.95–1.77 Ma) and decline during pre- and post-Olduvai times. Analogous lithological boundaries with ages are also shown.

gar section fall between ~2.7 (at base) and ~<0.5 (at top) Ma. We record Brunhes normal (<0.78 Ma), complete Matuyama reversal (2.58–0.78 Ma) and part of Gauss normal (>2.58 Ma) in the Ghaggar section. Matuyama includes Olduvai (1.95–1.77 Ma) and Reunion (2.15–2.14 Ma)

events (Figure 5). The palaeomagnetic sampling density was not achieved at ~700 to 800 m due to the predominance of conglomerates and friable nature of the rare mudstone and siltstone bed. This limited us to discover the minor events within the Matuyama, especially the Jaramilla event (1.070–0.990 Ma) for the Ghaggar river section. Since, there is no reversal after 0.78 Ma, the top of the section could not be constrained using magnetic polarity. However, from the minimum and maximum sediment accumulation rates of 42 cm/Ka and 62 cm/Ka in the Ghaggar river section, we could to estimate an age between 0.25 and 0.72 Ma for the top of the section at 1030 m (Figure 6). The average rate of sedimentation of 45 cm/Ka gives an age of 0.5 Ma (Figure 6).

*Sediment accumulation rate*

The average sediment accumulation rate for the Ghaggar section is ~45 cm/Ka and for the Moginand section ~26 cm/Ka (Figure 6). In the Ghaggar section, the rate of sedimentation is relatively less (47 cm/Ka) for the Pinjar Formation up to ~350 m and increases rapidly to 62 cm/Ka in the interval of 350–475 m stratigraphic level, corresponding to the Olduvai normal event (1.95–1.77 Ma; Figure 6). Thick conglomerate occurrences with immature and truncated palaeosols appear at ~455 m (1.77 Ma; Figure 2). The conglomerate comprising Tertiary clasts appears to be the result of the reactivation of the Nahar Thrust at 1.77 Ma. The rate of sedimentation drops to 42 cm/Ka



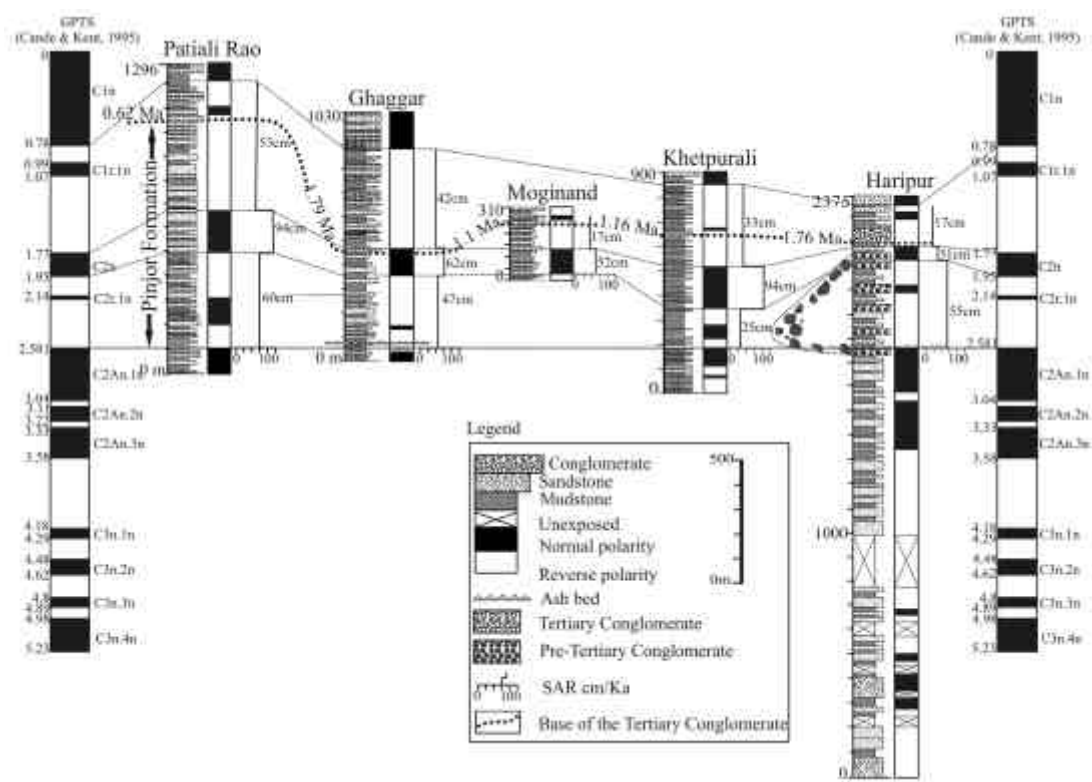


**Figure 7.** Correlation of five magnetostratigraphically dated sections from the Upper Siwalik Subgroup (Subathu sub-basin), and the time transgressive nature of the Boulder Conglomerate Formation marked at different time periods.

after Olduvai normal event (<1.77 Ma or 475 m) in the Ghaggar section (Figure 6). A similar drop in the rate of sedimentation in the Moginand section has been observed after Olduvai normal to 17 cm/Ka (Figure 7). Such a drop in the rate of sedimentation may be explained as depocentre progradation as a result of thrust loading. More detailed sedimentary–tectonic aspects will be published elsewhere.

**Regional stratigraphic correlation**

Five magnetostratigraphically constrained sections from the Subathu sub-basin (Patali Rao, Ghaggar, Moginand, Khetpurali and Haripur) are taken into account for regional correlation (Figures 1 and 7). The average rate of sedimentation for Patali Rao is 60 cm/Ka, for Ghaggar 45 cm/Ka, for Moginand 26 cm/Ka, for Khetpurali 37 cm/Ka and for Haripur section 32 cm/1000 years (Figure 7). Rapid rise in the Sediment Accumulation Rate (SAR) to 94 cm/1000 years (Patali Rao and Khetpurali) and 62 cm/Ka (Ghaggar) is observed during Olduvai times (1.95–1.77 Ma; Figure 7). Moreover, the conglomerates appeared earlier (1.76 Ma) at the eastern side of the basin (Haripur) and towards the west they become younger at Patali Rao (0.62 Ma). The average rate of sedimentation increases from 32 (at Haripur) to 60 cm/Ka (at Patali Rao). It is also interesting to note the basin-wide time-transgressive nature of the tertiary clast-bearing conglomerate. A detailed work on basin-wide

reconstruction of lithofacies and their relation to Himalayan tectono-climatic aspects is under progress.

**Conclusion**

The Ghaggar river section exhibits more than 1000 m of continuous sedimentary record characterizing the Pinjor type lithofacies and fauna. A fission track age of  $2.15 \pm 0.5$  Ma provides a benchmark and confirmation for the present magnetostratigraphic attempt in this section. Thus we provide magnetostratigraphic ages between 2.7 and 0.5 Ma for the Ghaggar section and 2 and 0.85 Ma for the adjacent Moginand section near Chandigarh. Further regional correlations for the Plio–Pleistocene formations of the Upper Siwaliks (Tatrot–Pinjor and Boulder Conglomerate Formations) in the study area have been achieved using magnetostratigraphy. The correlation suggests a highly time-transgressive nature of sedimentation and a regional drop in the rate of sedimentation after the termination of the Pinjor Formation (~1.77 Ma). With the availability of magnetostratigraphic ages in the Ghaggar section and successful correlation within the sub-basin, the Ghaggar section should be considered as a standard reference section for the Pinjor Formation.

1. Pilgrim, G. E., The correlation of the Siwaliks with the mammalian horizons of Europe. *Rec. Geol. Surv. India*, 1913, **43**, 264–325.



2. Ranga Rao, A., Nanda, A. C., Sharma, U. N. and Bhalla, Magnetic polarity stratigraphy of the Pinjor Formation (Upper Siwalik) near Pinjore, Haryana. *Curr. Sci.*, 1995, **68**, 1231–1236.
3. Tandon, S. K., Kumar, R., Koyama, M. and Niitsuma, N., Magnetic polarity stratigraphy of the Upper Siwalik Subgroup, east of Chandigarh, Punjab Sub-Himalaya, India. *J. Geol. Soc. India*, 1984, **25**, 45–55.
4. Sangode, S. J., Kumar, R. and Ghosh, S. K., Magnetic polarity of the Siwalik sequence of Haripur area (HP), NW Himalaya. *J. Geol. Soc. India*, 1996, **47**, 683–704.
5. Burbank, D. N., Beck, R. A. and Mulder, T., The Himalayan foreland basins. In *Tectonic Evolution of Asia* (eds Yin, A. and Harrison, T. M.), Cambridge University Press, 1996, pp. 149–188.
6. Parkash, B., Sharma, R. P. and Roy, A. K., The Siwalik Group (molasses) sediments shed by collision of continental plates. *Sediment. Geol.*, 1980, **25**, 127–159.
7. Tandon, S. K., The Himalayan Foreland: Focus on Siwalik Basin. In *Sedimentary Basins of India: Tectonic Context* (eds Tandon, S. K., Pant, C. C. and Casshyap, S. M.), Gyanodaya Prakashan, Nainital, 1991, pp. 177–201.
8. Pilgrim, G. E., Preliminary note on a revised classification of the tertiary freshwater deposits in India. *Rec. Geol. Surv. India*, 1910, **40**, 185–205.
9. Sahni, M. R. and Khan, E., Stratigraphy, structure and correlation of the Upper Shivaliks east of Chandigarh. *J. Palaeontol. Soc. India*, 1964, **4**, 59–72.
10. Sahni, A. and Mitra, H. C., Neogene palaeobiogeography of the Indian subcontinent with special reference to fossil vertebrates. *Palaeogeogr. Palaeoclimatol. Palaeoecol.*, 1980, **31**, 39–62.
11. Patnaik, R., Reconstruction of Upper Siwalik palaeoecology and palaeoclimatology using microfossil palaeocommunities. *Palaeogeogr. Palaeoclimatol. Palaeoecol.*, 2003, **197**, 135–150.
12. Nanda, A. C., Fossil equids from the Upper Siwalik Subgroup of the Ambala, Haryana. *Himalayan Geol.*, 1978, **8**, 149–177.
13. Raghavan, P., New records of microfossil assemblages from the Basal Pinjor Formation at Panchkula, Haryana (India). *Bull. Indian Geol. Assoc.*, 1990, **23**, 29–37.
14. Gaur, R. and Chopra, S. R. K., Taphonomy fauna, environment and ecology of Upper Siwaliks (Plio–Pleistocene) near Chandigarh, India. *Nature*, 1984, **308**, 353–355.
15. Ranga Rao, A., Magnetic polarity stratigraphy of Upper Siwalik of north-western Himalayan foothills. *Curr. Sci.*, 1993, **64**, 863–873.
16. Yokama, T., Palaeomagnetic study of Tatrot and Pinjor Formations, Upper Siwaliks, east of Chandigarh, northwest India. In *Proceedings: Neogene Quaternary Boundary Field Conference* (eds Sastry, M. V. A. *et al.*), 1979, Geological Survey of India, Calcutta, 1981, pp. 217–220.
17. Tandon, S. K. and Kumar, R., Discovery of tuffaceous mudstones in the Pinjor formation of Punjab sub-Himalaya, India. *Curr. Sci.*, 1984, **53**, 982–984.
18. Mehta, Y. P., Thakur, A. K., Nand Lal, Shukla, B. and Tandon, S. K., Fission track age of zircon separates of tuffaceous mudstones of the Upper Siwalik subgroup of Jammu–Chandigarh sector of the Punjab sub-Himalaya. *Curr. Sci.*, 1993, **64**, 519–521.
19. Kumar, R. and Tandon, S. K., Sedimentology of Plio–Pleistocene late orogenic deposits associated with intraplate subduction – The Upper Siwalik subgroup of a part of Panjab Sub-Himalaya, India. *Sediment. Geol.*, 1985, **105**, 1–59.
20. Raiverman, V. and Raman, Facies relations in the Subathu sediments, Simla Hills, northwestern Himalaya, India. *Geol. Mag.*, 1971, **108**, 329–341.
21. Viridi, N. S., On the dynamic significance of megalineaments in the outer and lesser regions of western Himalaya. *Himalayan Geol.*, 1979, **9**, 79–99.
22. Kumar, R., Ghosh, S. K., Sangode, S. J. and Thakur, V. C., Manifestation of intra-foreland thrusting in the Neogene Himalayan Foreland Basin fill. *J. Geol. Soc. India*, 2002, **59**, 547–560.
23. Kumar, R., Ghosh, S. K., Mazari, R. K. and Sangode, S. J., Tectonic impact on the fluvial deposits of Plio–Pleistocene Himalayan foreland basin, India. *Sediment. Geol.*, 2003, **158**, 209–234.
24. Collinson, D. W., *Methods in Rock Magnetism and Palaeomagnetism: Techniques and Instrumentation*, Chapman and Hall, London, 1987, pp. 189–205.
25. Butler, R. F., *Palaeomagnetism*, Blackwell, Oxford, 1992.
26. Cande, S. C. and Kent, D. V., Revised calibration of the geomagnetic polarity timescale for the Late Cretaceous and Cenozoic. *J. Geophys. Res. B*, 1995, **100**, 6093–6095.
27. Karunakaran, C. and Ranga Rao, A., Status of exploration for hydrocarbons in the Himalayan region – Contributions to stratigraphy and structure. *Geol. Soc. India, Misc. Publ.*, 1976, **41**, 1–66.
28. Raiverman, V., Kunte, S. V. and Mukherjee, A., Basin geometry, Cenozoic sedimentation and hydrocarbon prospects in northwestern Himalaya and Indo-Gangetic plains. *Petroleum Asia J.*, 1983, **6**, 67–92.
29. Powers, P. M., Lillie, R. J. and Yeats, R. S., Structure and shortening of the Kangra and Dehra Dun reentrants, Sub-Himalaya, India. *Geol. Soc. Am. Bull.*, 1998, **110**, 1010–1027.

ACKNOWLEDGEMENTS. This work was carried out under the research grant (ESS/23/VES/146/2001) funded by Ministry of Science and Technology, New Delhi. We thank the Director, Wadia Institute of Himalayan Geology (WIHG), Dehra Dun for encouragement and providing facilities to carry out this work. We also thank Mr Rakesh Kumar, Palaeomagnetic Laboratory, WIHG for assisting in analytical work.

Received 28 July 2004; revised accepted 24 December 2004